JPE 9-5-11

A Novel Soft-Switching Two-Switch Flyback Converter with a Wide Operating Range and Regenerative Clamping

Marn-Go Kim† and Young-Seok Jung*

†Division of Electrical and Control Eng., Pukyong National University, Busan, Korea
*Division of Mechanical Eng., Pukyong National University, Busan, Korea

ABSTRACT

A novel soft-switching two-switch flyback converter is proposed in this paper. This converter is composed of two active power switches, a flyback transformer, a blocking diode, and two passive regenerative clamping circuits. The proposed converter has the advantages of a low cost circuit configuration, a simple control scheme, a high efficiency, and a wide operating range. The circuit topology, analysis, design considerations, and experimental results of the new flyback converter are presented.

Keywords: Two-switch flyback converter, Soft switching, Regenerative clamping, Power factor correction

1. Introduction

Flyback converters are popular topologies widely used in isolated DC-DC power converters[1-4]. These topologies are favored by designers for their simplicity, ability to handle multiple isolated outputs, and the ease of optimizing their duty cycle by selecting the transformer turns ratio. The simplicity is partially based on the fact that conventional flyback converters employ a single MOSFET switch, which is primary ground referenced for convenient gate drive implementation.

However, the drawback to this single switch approach is that the voltage stress on the switch is the sum of the input voltage, the reflected transformer voltage and the turn-off voltage spike caused by leakage inductance. A common problem with flyback converters is the leakage inductance of the power transformer, which causes high turn-off voltage spikes. This problem is particularly serious at high line voltage or at light loads[5].

Adding a second MOSFET switch on the high side results in a two-switch flyback topology, where the voltage stress on each MOSFET is clamped to the input voltage. The leakage inductance energy is also clamped and recycled back to the input to improve efficiency. The dissipative snubber circuit that is often required in a single switch approach is no longer required. MOSFET switches with a rated voltage slightly higher than the input voltage can be employed in the two-switch topology, while a rating of greater than twice the input voltage is required for a single-switch topology. For many applications the added complexity and increased part count of two-switch

Manuscript received Jan. 13, 2009; revised July 29, 2009.
†Corresponding Author: mgkim@pknu.ac.kr
Tel: +82-51-629-6330, Fax: +82-51-629-6305, PKNU
Division of Electrical and Control Eng., Pukyong Nat'l Univ. Busan, Korea
*Division of Mechanical Eng., Pukyong Nat'l Univ. Busan, Korea

flyback converters is a small price to pay for the benefits received.

However, the duty ratio of a conventional two-switch topology cannot be more than 50%, which is the same disadvantage as a conventional two-switch forward one[6,7]. The reset voltage of the transformer can't be more than the input voltage because there are two diodes D_3 and D_4 as shown in Fig. 1, which clamp the transformer primary voltage to the input voltage. When the reflected output voltage to the transformer's primary side is higher than the input voltage, most of the magnetizing inductor energy as well as the leakage inductor energy is returned to the input source. In addition, the converter is operated under a hard switching condition. Because of these disadvantages, it cannot be used for power factor correction (PFC) applications[8,9].

In order to overcome these problems, a novel soft-switching two-switch flyback converter with a wide operating range and regenerative clamping is proposed in this paper. Due to its simple circuit configuration, consisting of a minimum number of components and since only passive components are utilized in the clamping circuit to achieve zero voltage soft switching, the proposed converter can be controlled by a single PWM signal, establishing a low-cost circuit configuration and a simple control scheme. The duty ratio of the proposed converter can be more than 50%, and magnetizing inductor energy transfer to the transformer's secondary side is possible even if the reflected output voltage is higher than the input voltage.

In Section 2 the limitations of the operation range in a conventional two-switch flyback converter will be discussed. In Section 3 a detailed analysis of the proposed topology will be carried out. In Section 4 the experimental results will be given.

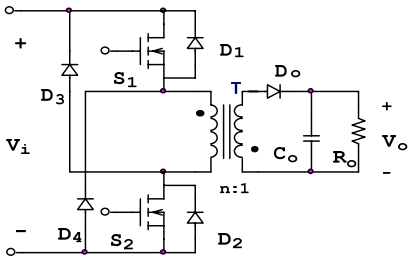

Fig. 1. Conventional two-switch flyback converter.

2. Limitations of Operation Range in Conventional Two-switch Flyback Converter

In a continuous conduction mode(CCM) of operation, the output voltage of Fig. 1 is given by:

$$nV_o = \frac{D}{1-D}V_i \tag{1}$$

where n is the transformer turns ratio and D is the duty ratio. If the efficiency of the flyback converter is 1, the output power in discontinuous conduction mode(DCM) can be expressed as:

$$P_o = \frac{L_1 I_p^2}{2} f_s = \frac{V_o^2}{R_o} \tag{2}$$

$$I_p = \frac{V_i}{L_1} DT_s = \frac{V_i}{f_s L_1} D \tag{3}$$

where L_1 = primary magnetizing inductance, I_p = peak current of L_1, f_s = switching frequency, R_o = load resistance, D = duty ratio and T_s = switching period. From (2) and (3), the output voltage in DCM is given by:

$$V_o = \frac{DV_i}{\sqrt{2 f_s L_1 / R_o}} \tag{4}$$

In Fig. 1, both switches are turned on and off simultaneously, as in the two-switch forward converter. The operation of the flyback transformer is best described as a two-winding coupled inductor. Energy is supplied to

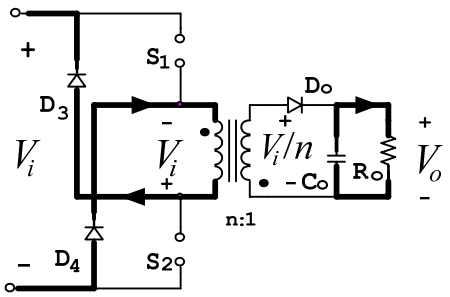

Fig. 2. Energy returning mode of Fig. 1 ($nV_o > V_i$).

the inductor in the primary circuit when the primary switches S_1 and S_2 are active, then the energy is released to the secondary when the primary switches are turned off if the reflected transformer primary voltage nV_o is lower than the input voltage V_i. However, this energy is returned to the input source if nV_o is higher than V_i as shown in Fig. 2. In the steady-state, nV_o needs to be lower than V_i in order to transfer the magnetizing energy to the secondary output in a conventional two-switch topology. Therefore, from (1) and (4), the limitations in operation range of Fig. 1 can be calculated as:

$$D<0.5 \quad \text{for CCM}$$

$$\text{and} \quad D<\sqrt{2 f_s L_1/(n^2 R_o)} \quad \text{for DCM} \tag{5}$$

3. Proposed Two-switch Flyback Converter

3.1 Circuit Description

The circuit of the proposed two-switch flyback converter is illustrated in Fig. 3. This converter is composed of two active power switches (S_1, S_2), a flyback transformer T, a blocking diode D_b, and two passive regenerative clamping circuits that consist of two diodes (D_3, D_4), two inductors (L_{s1}, L_{s2}), two capacitors (C_{s1}, C_{s2}) and a diode D_P. The diode D_P is used to trap leakage inductor energy into C_{s1} and C_{s2} when the two switches are turned off, and then regenerate the energy to the input V_i. The diode D_b is inserted to suppress resonance between the transformer inductor and the capacitors around it. In addition, inserting D_b provides zero voltage switching for S_1 and S_2 when the two switches are turned off. Thus, the reduced switching losses of S_1 and S_2 cancel out the conduction loss of D_b.

3.2 Circuit Operation

Fig. 4 shows the operating modes of the proposed

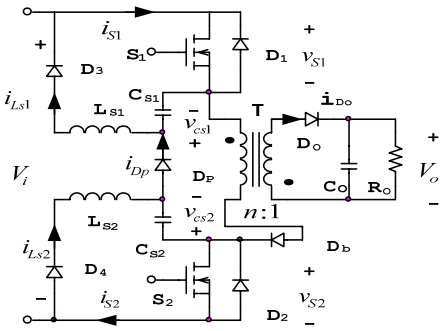

Fig. 3. Proposed two-switch flyback converter.

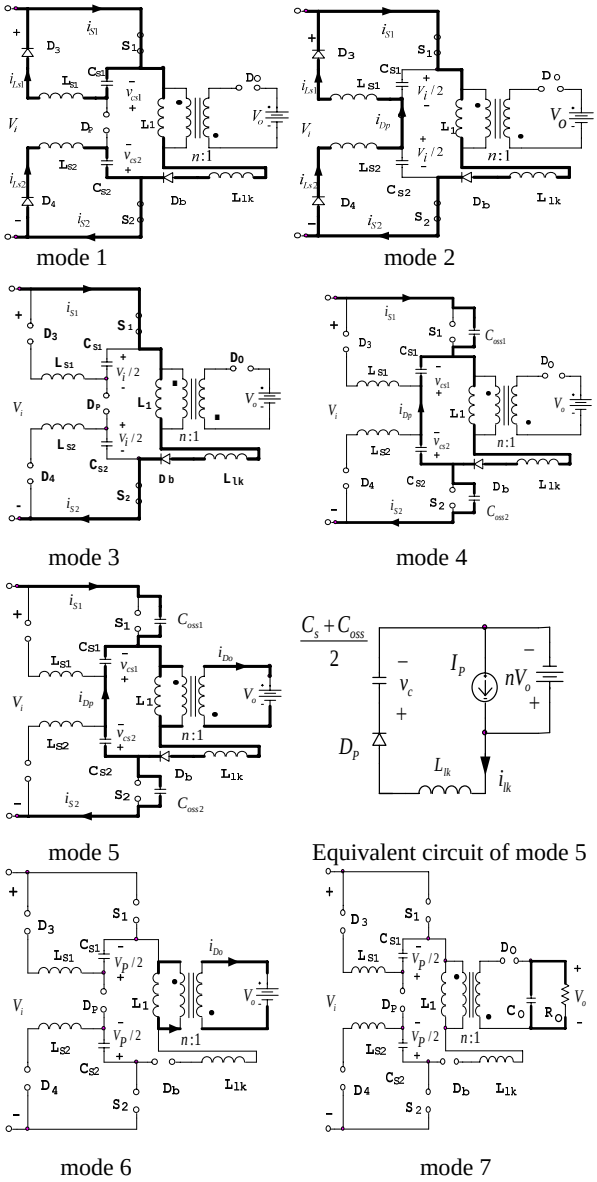

Fig. 4. Operating modes of Fig. 3.

converter under steady-state, where the following assumptions are made:

1) All switching components are ideal.
2) The inductors L_{s1} and L_{s2} are identical, $L_{s1}=L_{s2}=L_s$.
3) The capacitors C_{s1} and C_{s2} are identical, $C_{s1}=C_{s2}=C_s$.
4) The switch output capacitors are identical, $C_{oss1}=C_{oss2}=C_{oss}$.
5) The output voltage ripple can be neglected.
6) The converter is operating in DCM.

Typical voltage and current operating waveforms for the proposed circuit topology are illustrated in Fig. 5. The steady-state operation of this circuit can be described as follows:

Mode 1 (t_0–t_1): At time t_0, according to the duty factor D of the power converter treated here, S_1 and S_2 are turned on simultaneously under a zero current condition. The primary side of the transformer is clamped by input voltage. The primary current circulates through S_1 and S_2 and increases linearly. Partial resonance based on L_s and C_s begins. Assuming that $v_{cs}(0)=V_P/2, i_{Ls}(0)=0$,

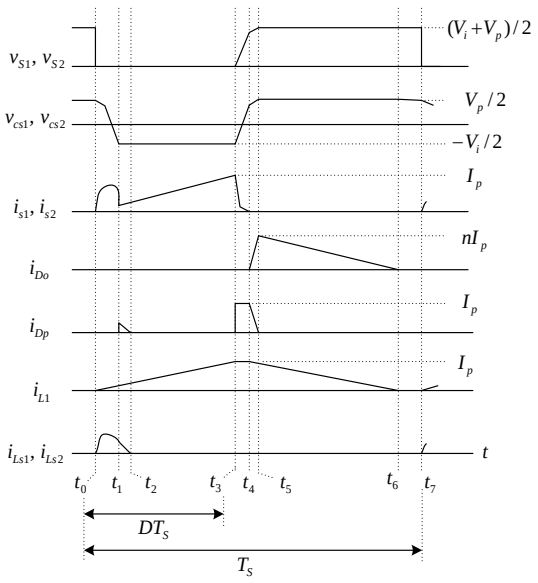

Fig. 5. Key theoretical waveforms of proposed converter.

the equations for the resonant inductor current and capacitor voltage during this operation mode can be expressed as:

$$i_{Ls}=\frac{V_P}{2Z_s}\sin w_s(t-t_0)$$
$$v_{cs}=\frac{V_P}{2}\cos w_s(t-t_0) \quad (6)$$

where $w_s=1/\sqrt{L_sC_s}$ is the resonant angular frequency and $Z_s=\sqrt{L_s/C_s}$ is the characteristic impedance.

On the other hand, the current through S_1 and S_2 can be derived from the flyback transformer's primary side current and resonant inductor current. Therefore, the active power switch current can be represented as:

$$i_s=\frac{V_i}{L_1+L_{lk}}(t-t_0)+\frac{V_P}{2Z_s}\sin w_s(t-t_0) \quad (7)$$

Mode 2 (t_1–t_2): Initially, at t_1, v_{cs} equals $-V_i/2$ and i_{Ls} equals $\frac{V_P}{2Z_s}\sin w_s(t_1-t_0)$. The diode D_P is turned on to provide a path for the regeneration current. For energy recovery, current i_{Ls} flows through the current regeneration loop composed of D_3, D_4, D_P, L_{s1}, L_{s2} and V_i. The regeneration current can be represented as:

$$i_{Ls}(t)=\frac{V_P}{2Z_s}\sin w_s(t_1-t_0)-\frac{V_i}{2L_s}(t-t_1) \quad (8)$$

The flyback transformer's primary side current flows through the active power switches. The capacitor voltage v_{cs} is clamped at $-V_i/2$ and the regeneration current i_{Ls} is decreased towards zero.

Mode 3 (t_2–t_3): In this mode, the magnetizing

inductance L_1 and the leakage inductance L_{lk} are charged up linearly by the input voltage source V_i. At t_3, the peak transformer's primary side current can be given by:

$$I_P = \frac{V_i}{L_1 + L_{lk}}(t_3 - t_0) \cong \frac{V_i}{L_1} DT_s = \frac{DV_i}{f_s L_1} \quad (9)$$

where $T_s = 1/f_s$.

Mode 4 (t_3–t_4): According to the duty factor D, at t_3, S_1 and S_2 are turned off simultaneously under zero voltage soft switching. The diode D_P begins to conduct. The output capacitor of the active power switches C_{oss} is charged and the voltage across the switches increases linearly with a certain slope. The voltage across C_s is linearly changed from $-V_i/2$ to $nV_o/2$. The voltage across the active switches and the voltage across C_s are given by:

$$v_s = \frac{I_P}{C_s + C_{oss}}(t - t_3)$$

$$v_{cs} = -\frac{V_i}{2} + \frac{I_P}{C_s + C_{oss}}(t - t_3) \quad (10)$$

Mode 5 (t_4–t_5): At t_4, $2v_{cs}$ is equal to nV_o and the output diode D_o begins to conduct. The output current starts to increase and the leakage inductor current begins to decrease. From the equivalent circuit of mode 5, the equations for the leakage inductor current and the capacitor voltage can be expressed as:

$$i_{lk} = I_P \cos w_k (t - t_4)$$

$$v_c = 2v_{cs} = Z_k I_P \sin w_k (t - t_4) + nV_o \quad (11)$$

where $w_k = 1/\sqrt{L_{lk}(C_s + C_{oss})/2}$ and $Z_k = \sqrt{2L_{lk}/(C_s + C_{oss})}$.

At t_5, i_{lk} drops to zero and the peak capacitor voltage is given by:

$$V_P = Z_k I_P + nV_o \quad (12)$$

Substituting (4) and (9) into (12) gives:

$$V_P = \left(\frac{Z_k}{f_s L_1} + \frac{n}{\sqrt{2 f_s L_1 / R_o}}\right) DV_i \quad (13)$$

The maximum off-state voltage across the active switches S_1 and S_2 is given by:

$$V_{s1,\max} = V_{s2,\max} = (V_i + V_P)/2 \quad (14)$$

Mode 6 (t_5–t_6): At t_5, i_{lk} drops to zero. All the remaining magnetizing current flows into the output. The voltage across the primary side of the transformer is nV_o.

Mode 7 (t_6–t_7): The magnetizing current in the secondary winding reduces to zero at t_6. The output capacitor is discharged through the load resistance. Switches S_1 and S_2 are turned on at t_7 to start the next switching cycle.

4. Experimental Results

4.1 Design Considerations

Practical conditions must be met in order to select optimum parameters. To achieve zero voltage switching when S_1 and S_2 are turned off, V_P should be higher than V_i. Using (13), this is given by:

$$\left(\frac{Z_k}{f_s L_1} + \frac{n}{\sqrt{2 f_s L_1 / R_o}}\right) D > 1 \quad (15)$$

The minimum on-time of active switches S_1 and S_2 is to

be longer than the full discharging interval of capacitors C_{s1} and C_{s2}:

$$\pi\sqrt{L_s C_s} < D_{\min} T_s . \quad (16)$$

From (10), the maximum dv/dt during turn-off of active power switches should be $\frac{I_P}{C_s + C_{oss}}$. Finally, from (7), the maximum di/dt during turn-on of active power switches should be $\frac{V_P}{2L_s} + \frac{V_i}{L_1 + L_{lk}}$.

4.2 Experimental Evaluations

To determine the feasibility of the proposed soft-switching two-switch flyback converter, a prototype of the circuit shown in Fig. 3 was built according to the following specifications:

Input voltage: 200 V.

Output voltage: 80 V.

The following are the circuit parameters used in the experiment:

$f_s = 35\,kHz$, $n = 2.4$, $L_1 = 1.33\,mH$, $L_{lk} = 38\,\mu H$, $C_{s1} = C_{s2} = 4.4\,nF$, $L_{s1} = L_{s2} = 200\,\mu$H. For S_1 and S_2, an IRF 840 is used. For D_b, D_3, and D_4, a DSEI 12-06A is used. And a DSEI 30-10A is used for D_o and D_p.

Fig. 6 shows the coupled inductor used to implement L_{s1} and L_{s2}. The primary and secondary inductances of the coupled inductor are 100 uH, respectively, to effectively achieve the experimental two 200 uH inductors. The control circuit is shown in Fig. 7. Gate signals V_{g1}, V_{g2} are generated in order to control the two transistors S_1, S_2.

The experimental voltage and current waveforms of the active power switch S_2 are illustrated in Fig. 8 for D=0.41. From equations (9) and (12), the peak transformer's primary side current I_P and the peak capacitor voltage V_P are 1.76 A and 423 V, respectively. From (14),

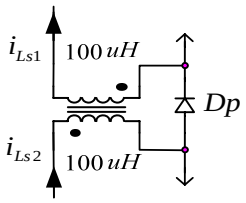

Fig. 6. Implemented circuit of L_{s1} and L_{s2}.

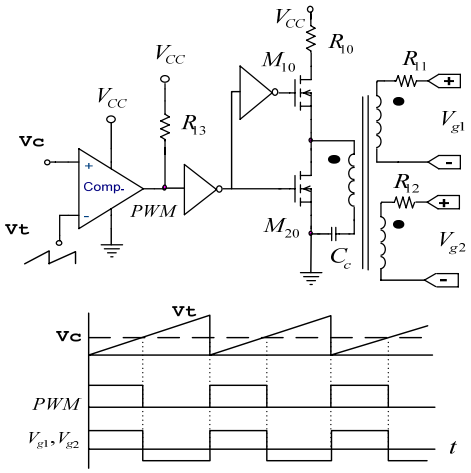

Fig. 7. Control Circuit and related waveforms.

the maximum off-state voltage across switch S_2 is 311.5 V. From the experimental waveforms, the active switch turns on under a zero current condition and turns off under a zero voltage condition. The experimental waveforms show excellent agreement with the theoretical results.

The experimental voltage across C_{s2} and current through D_p are illustrated in Fig. 9. From Fig. 5, the theoretical peak positive and negative values of V_{cs2} are 211.5(=$V_P/2$) V and -100 V (=$-V_i/2$), respectively. From the i_{Dp} waveform, we can see the regeneration current after V_{cs2} reaches -100 V. Fig. 10 shows the experimental waveforms of V_{cs2} and i_{Ls2}. From (6), Z_s is 213 Ω and the peak value of the resonant current is 0.99 A.

Fig. 11 shows the experimental voltage waveforms across S_1, S_2, C_{s1}, and C_{s2}. From the experiment, it can be verified that V_{s1} and V_{cs1} are identical to

V_{s2} and V_{cs2}, respectively. Fig. 12 shows the voltage across S_2 and the current through output diode D_o. These experimental results confirm the theoretical waveforms illustrated in Fig. 5.

In Fig. 13, the measured efficiency of the proposed converter as a function of output power is represented. The maximum efficiency obtained from this flyback converter is 92.5 %. Fig. 14 shows the experimental line voltage and current waveforms. The measured input power factor is 0.98.

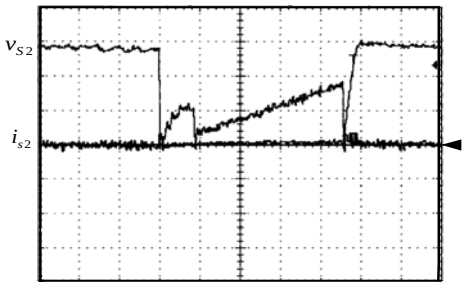

Fig. 8. Experimental waveforms : v_{s2} (100 V/div) and i_{s2} (1 A/div), time: 2.5 μs /div.

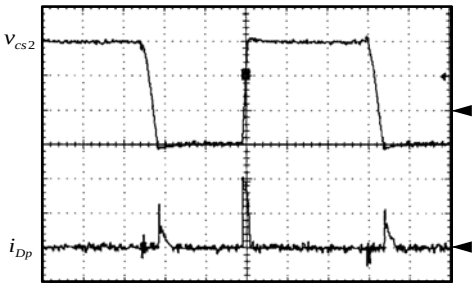

Fig. 9. Experimental waveforms : v_{cs2} (100 V/div) and i_{Dp} (1 A/div), time: 5 μs /div.

Fig. 10. Experimental waveforms : v_{cs2} (100 V/div) and i_{Ls2} (1 A/div), time: 5 μs /div.

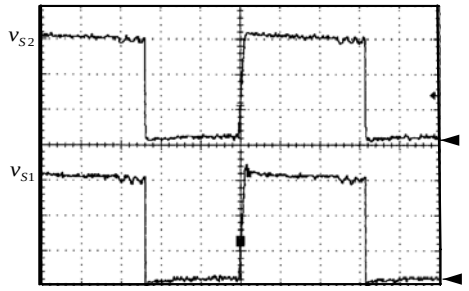

(a)

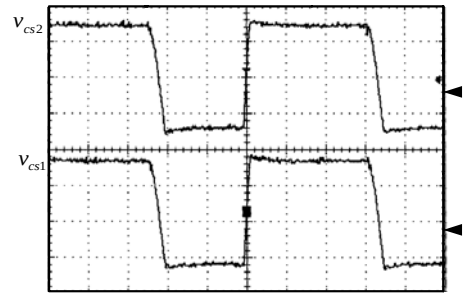

(b)

Fig. 11. Experimental waveforms : (a) v_{s1} and v_{s2} (100 V/div) (b) v_{cs1} and v_{cs2} (100 V/div), time: 5 μs /div.

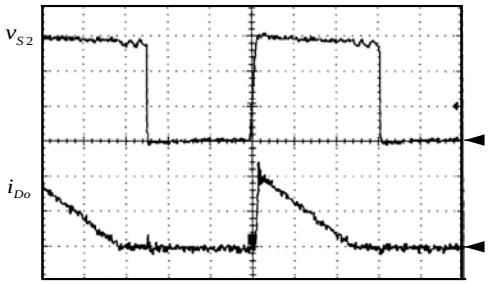

Fig. 12. Experimental waveforms : v_{s2} (100 V/div) and i_{Do} (2 A/div), time: 5 μs /div.

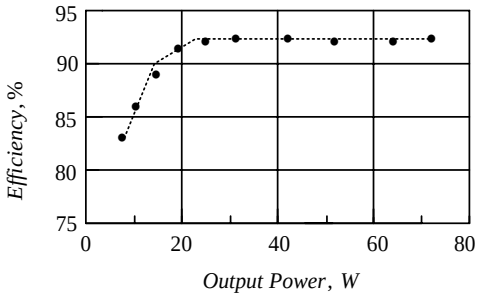

Fig. 13. Measured efficiency as a function of the output power when $V_i = 200V$ and $V_o = 80V$.

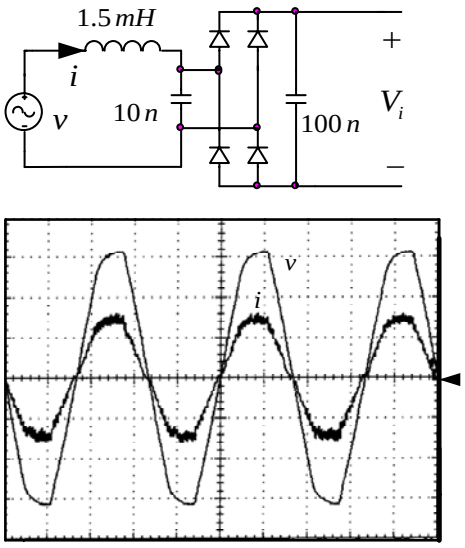

Fig. 14. Line voltage and current waveforms . Outer trace: line voltage at 100 V/div; inner trace: line current at 0.2 A/div. Time base is 5 *ms* /div.

5. Conclusions

A novel soft-switching two-switch flyback converter with a wide operating range and regenerative clamping is proposed. The voltage stress on each main switch is clamped to a limited level. The leakage inductance energy is also clamped and recycled back to the input to improve efficiency. Due to its simple circuit configuration, consisting of a minimum number of components and since only passive components are utilized in the clamping circuit to achieve zero voltage soft switching, the proposed converter can be controlled by a single PWM signal, establishing a low-cost circuit configuration and a simple control scheme. The duty ratio of the proposed converter can be more than 50%, and the magnetizing inductor energy transfer to the transformer's secondary side is possible even if the reflected output voltage is higher than the input voltage. A detailed analysis and the design and implementation of the circuit have also been discussed. Experimental results have demonstrated that the proposed converter can function very efficiently as a PFC circuit.

References

[1] T. Ninomia, T. Tanaka, and K. Harada, "Analysis and optimization of a nondissipative LC turn-off snubber," *IEEE Trans. Power Electron.*, Vol. 3, no. 2, pp. 147-156, Apr. 1988.

[2] F. Tsai, P. Markowski, and E. Whitcomb, "Off-line flyback converter with input harmonic current correction," *in Proc. IEEE-INTELEC'96*, pp. 120-124, 1996.

[3] B. Singh and G.D. Chaturvedi, "Analysis, Design and Development of a Single Switch Flyback Buck-Boost AC-DC Converter for Low Power Battery Charging Applications," *Journal of Power Electronics*, Vol. 7, no. 4, pp.318-327, 2007.

[4] B.H. Lee, C.E. Kim, K.B. Park, and G.W. Moon , "A New Single-Stage PFC AC/DC Converter with Low Link-Capacitor Voltage," *Journal of Power Electronics*, Vol. 7, no. 4, pp. 328-335, 2007.

[5] Q. Zhao, F.C. Lee, and F. Tsai, "Voltage and current stress reduction in single-stage power factor correction AC/DC converters with bulk capacitor voltage feedback," *IEEE Trans. Power Electron.*, Vol. 17, no. 4, pp. 477-484, July 2002.

[6] Y. Gu, X. Gu, L. Hang, Z. Lu, and Z. Qian, "Improved wide range dual switch flyback dc/dc converters," *in Proc. IEEE-APEC'04*, pp. 654-658, 2004.

[7] Y. Wei, X. Wu, Y. Gu, and H. Ma, "Wide range dual switch forward-flyback converter with symmetrical RCD clamp," *in Proc. IEEE-PESC'05*, pp. 420-424, 2005.

[8] K.W. Siu and Y.S. Lee, "A novel high-efficiency flyback power-factor-correction circuit with regenerative clamping and soft switching," *IEEE Trans. Circuits Syst. I*, Vol. 47, pp. 350-356, Mar. 2000.

[9] J. Zhao and F. Dai, "Soft-switching two-switch flyback converter," *in Proc. IEEE-ICIEA'08*, pp. 250-254, 2008.

Marn-Go Kim received a B. S. degree in electrical engineering from Kyungpook National University in 1986, and his M. S. and Ph.D. in electrical engineering from Korea Advanced Institute of Science and Technology in 1988 and 1991, respectively. From 1991 to 1994, he was with the Korea Telecom Research Center, where he worked on the research of telecom power systems such as uninterruptible power supplies, DC/DC converters and distributed power systems. Since 1995, he has been with the Department of Control and Automation Engineering, Pukyong National University, where he is now a professor. His research interests include the modeling, analysis, and control of resonant converters, power semiconductor circuits, and soft switching converters. Dr. Kim is a member of KIPE and KIEE.

Young-Seok Jung received his B.S., M.S. and Ph.D. in Electrical Engineering from the Korea Advanced Institute of Science and Technology (KAIST), Daejon, Korea, in 1992, 1994, and 1999, respectively. He worked for the Hyundai Autonet, Powertrain Team, from 1999 to 2002. Since 2002, he has been with the Division of Mechanical Engineering at Pukyong National University, Korea. His research interests are in the areas of power converters and variable speed motor drives. Dr. Jung is a member of the Korean Institute of Power Electronics (KIPE).